

## A $K=3$ two-quasiparticle isomer in $^{98}\text{Sr}$

G. Lhersonneau,<sup>1,\*</sup> B. Pfeiffer,<sup>2</sup> R. Capote,<sup>3,4</sup> J. M. Quesada,<sup>3</sup> H. Gabelmann,<sup>2,†</sup> K.-L. Kratz,<sup>2</sup>  
and the ISOLDE Collaboration<sup>5</sup>

<sup>1</sup>*Department of Physics, University of Jyväskylä, P.O. Box. 35, FIN-40351 Jyväskylä, Finland*

<sup>2</sup>*Institut für Kernchemie, Universität Mainz, D-55128 Mainz, Germany*

<sup>3</sup>*Departamento de Física Atómica, Molecular y Nuclear, Universidad de Sevilla, Facultad de Física, Apdo 1065, 41080 Sevilla, España*

<sup>4</sup>*Centro de Estudios Aplicados al Desarrollo Nuclear, Apdo 100, Miramar, La Habana, Cuba*

<sup>5</sup>*CERN, CH-1211 Geneva 23, Switzerland*

(Received 17 September 2001; published 25 January 2002)

The decay of on-line mass-separated  $^{98}\text{Rb}$  to  $^{98}\text{Sr}$  is studied by  $\gamma$  spectroscopy. The revised decay scheme adds further evidence of the coexistence of very different shapes in  $^{98}\text{Sr}$ . A set of levels is proposed to originate from particle-hole pair excitations across the  $Z=40$  spherical gap in analogy with  $^{96}\text{Sr}$ . A deformed  $K=3$  band with probable even parity is built on a 7.1-ns isomer at 1838 keV. It is interpreted as a two-quasineutron excitation in accordance with a quantum Monte Carlo pairing calculation based on a deformed shell model. Configurations of the calculated lowest-lying two-quasiparticle levels confirm the importance of the  $[404]9/2$  neutron orbital at the largest deformations in the neutron-rich  $A \approx 100$  region.

DOI: 10.1103/PhysRevC.65.024318

PACS number(s): 23.20.-g, 21.10.-k, 27.60.+j

### I. INTRODUCTION

Neutron-rich nuclei in the  $A \approx 100$  region exhibit a number of interesting features including shell-closure effects near the crossing of the  $Z=40$  and  $N=56$  spherical subshells and the occurrence of large ground-state deformations for  $N \geq 60$ . In strontium ( $Z=38$ ) and zirconium ( $Z=40$ ) isotopes, deformed levels have been identified for  $N \geq 58$ . With increasing neutron number, they rapidly become lower in energy from about 1.5 MeV in  $^{96}\text{Sr}$  and  $^{98}\text{Zr}$  [1], while there are indications that deformations increase [2]. The  $N=60$  isotones  $^{98}\text{Sr}$  and  $^{100}\text{Zr}$  are rare examples of the coexistence of very different nuclear shapes at nearly the same energy. The first excited  $0^+$  states lie at only 216 and 331 keV, respectively [3,4]. Whereas these states are interpreted as spherical or only slightly deformed, large deformations of  $\beta \approx 0.40$  have been measured for the ground states (g.s.'s) [5–7]. These cases of shape coexistence were also discussed in a more general context by Wood *et al.* [8]. The g.s. bands were recently extended to higher-spin members by prompt fission experiments [9–11]. However, the nature of most excited states in  $^{98}\text{Sr}$  and  $^{100}\text{Zr}$  is still unclear.

Large deformations in this region favor the occurrence of isomers due to  $K$  hindrance. Thus, in the odd-proton ( $Z=39$ ) and  $N=60$  nucleus  $^{99}\text{Y}$ , a 8.6- $\mu\text{s}$   $I^\pi = 17/2^+$  isomer was discovered at the gas-filled mass separator JOSEF [12]. This was the first opportunity to observe extended band structure in this region. More recently, a  $K^\pi = 5^-$  or  $6^+$  excited band was observed in  $^{100}\text{Zr}$  in prompt-fission experiments [9–11]. Other two-quasiparticle band heads were observed in  $N=62$  isotones. A 85-ns isomer in  $^{100}\text{Sr}$  [13] and a band head in  $^{102}\text{Zr}$  [9–11] were interpreted as being based on a  $4^-$  two-quasineutron pair. These observations give insight into the nature of quasiparticle levels and into the pairing

strength. From general features of  $\beta$ -decay properties [14,15], together with calculations of the energies of two-quasiparticle states [16] and an analysis of extended band structures [9–11,17], it was concluded that pairing in this region is considerably lower than the standard estimate.

In an analysis of new  $\beta$ -decay data, the 1838-keV level in  $^{98}\text{Sr}$  was found to be an isomer with a 7.1-ns half-life [18]. However, it could not be interpreted in the context of the level scheme of Ref. [3]. By analogy, another isomeric level could have been expected in  $^{100}\text{Zr}$ . However, no such level was reported in the  $\beta$  decay of  $^{100}\text{Y}$  [4]. These considerations motivated investigations of the decay schemes of  $^{98}\text{Rb}$  to  $^{98}\text{Sr}$  and of  $^{100}\text{Y}$  to  $^{100}\text{Zr}$ , the results of which are reported in this paper.

### II. EXPERIMENTS

The data for  $^{98}\text{Sr}$  were obtained during the course of the measurement devoted to  $^{100}\text{Sr}$  reported in Ref. [19] and details can be found there. In short, the parent nucleus  $^{98}\text{Rb}$  was obtained at the ISOLDE facility as a product of the fission of  $^{238}\text{U}$  by 600-MeV protons, followed by an on-line mass-separation. The implantation spot was viewed by a planar Ge detector, a large coaxial Ge detector, and a  $\text{BaF}_2$  scintillator. This experiment did not basically differ from the former one at the mass-separator OSTIS at the high-flux reactor of the ILL-Grenoble [3], except for the production mode. The Ge detectors were placed quite far, at about 10 cm, from the source. Coincidence summing was therefore negligible, and only few cross-talks were observed in the coincidence spectra. In spite of lower statistics, the superior energy resolution of the planar detector improved the analysis of the complex region below 300 keV. This revealed new coincidence relationships of particular importance for a revision of the decay scheme. The dedicated lifetime measurement of the  $2^+$  state has been reported in Ref. [19]. We investigated other levels using  $\gamma$ - $\gamma$ - $t$  coincidences with Ge-detectors. In case of high-lying levels, in order to increase

\*Present address: LNL-INFN, Legnaro, Italy.

†Present address: KSM-Analytik, Mainz, Germany.

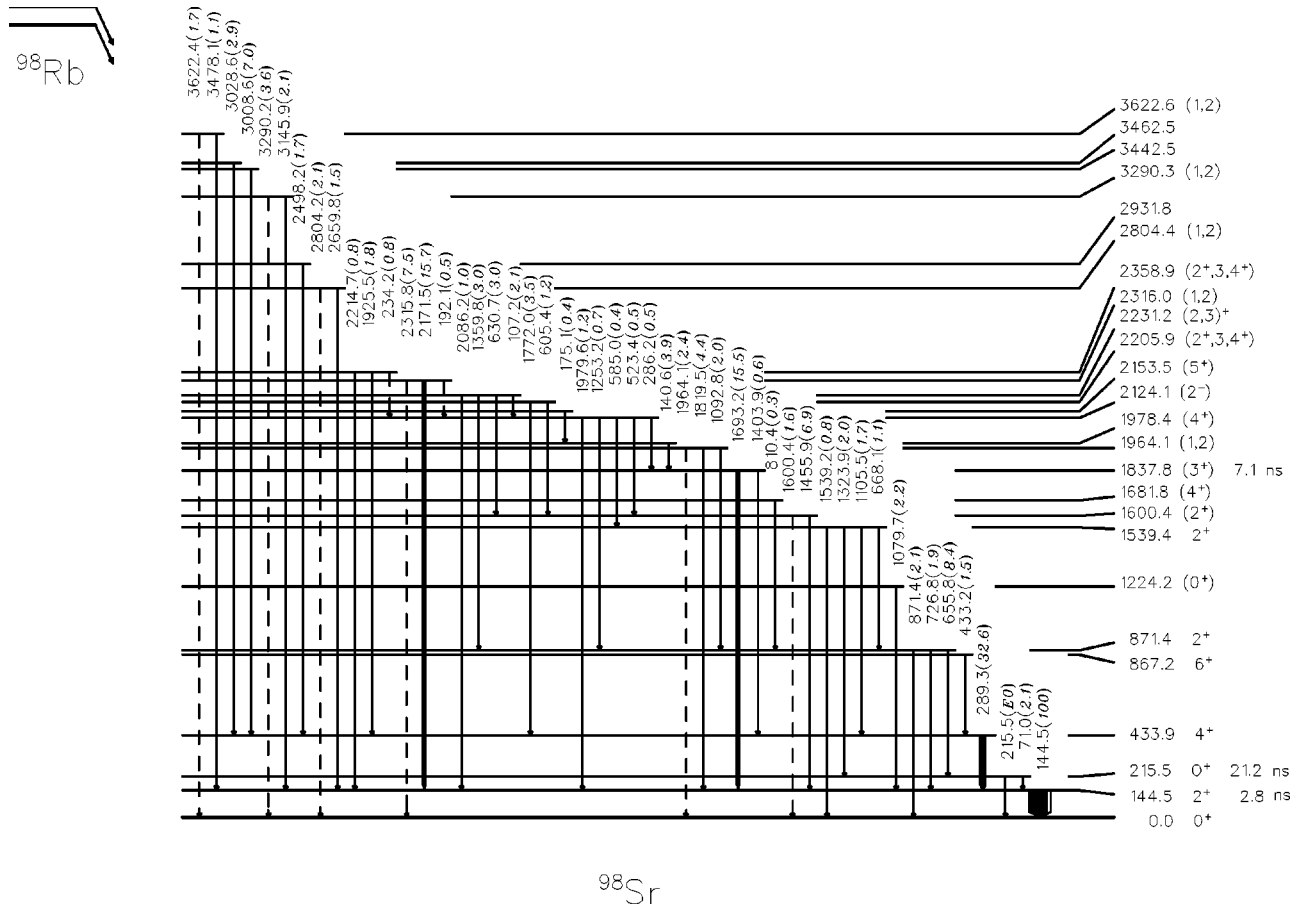


FIG. 1. Levels in  $^{98}\text{Sr}$  populated by  $\beta$  decay of  $^{98}\text{Rb}$ . The decomposition of feedings in ground state and isomer decays is discussed in the text. An example of the calculation of branchings and logft values is shown in Table III, where  $I^\pi=3^+$  has been assumed for the higher-spin  $^{98}\text{Rb}$  level.

statistics a gate was set on a depopulating transition, carefully correcting for Compton events below the peak, while the other time channel accepted a wide range of energies. A threshold was introduced to suppress the interference of levels with known lifetimes. As in standard  $\beta$ - $\gamma$ - $t$  coincidences, disturbances of the time distributions by occasional higher-lying long-lived levels can occur. The validity of the measurement was checked by a systematic analysis of time spectra for all sufficiently strong transitions.

The  $\gamma$ - $\gamma$  coincidence data for  $^{100}\text{Zr}$  were obtained at the IGISOL separator [20] during a short test run. An energy-energy matrix was formed by combining data from four Ge detectors with 70% efficiency. The parent nucleus  $^{100}\text{Y}$  was produced by 25-MeV  $p$ -induced fission of  $^{238}\text{U}$ , and delivered to the collection station as a beam together with other isobaric activities. Since the beam contains low and high-spin  $^{100}\text{Y}$  levels, it is possible to access medium spin  $^{100}\text{Zr}$  levels after  $\beta$  decay. This was not possible in the previous decay studies at TRISTAN where, due to the chemical selectivity of the ion source,  $^{100}\text{Y}$  was obtained as a  $\beta$ -decay daughter of mass separated  $^{100}\text{Sr}$  only populating the low-spin levels [4]. These data thus fill the gap between low-spin levels observed in the former decay studies and the higher-spin ones populated in prompt fission.

### III. RESULTS

#### A. Level scheme of $^{98}\text{Sr}$

The decay scheme of  $^{98}\text{Rb}$  is shown in Fig. 1, and transitions are listed in Table I. The quoted intensities are the observed ones, as they result from the superposition of the decays of the low spin  $I=(0,1)$ ,  $T_{1/2}=116$  ms, and higher spin  $T_{1/2}=96$  ms isomers of  $^{98}\text{Rb}$  [21]. It is not possible to disentangle these contributions by using decay curves, due to their very close half-lives. In a later section, we present a decomposition of the feeding intensities on the basis of level spin differences. The intensity ratio  $I_\gamma(4^+ \rightarrow 2^+)/I_\gamma(2^+ \rightarrow 0^+)=0.32$  is the same as in experiments performed with thermal neutrons [22,23]. This can be interpreted in two ways. This ratio remains the same if the  $2^+$  and  $4^+$  states in  $^{98}\text{Sr}$  are populated by the high-spin decay only, which could give some constraints on the  $^{98}\text{Rb}$  ground-state and isomer spins. Alternatively, it could be that the relative populations of  $^{98}\text{Rb}$  g.s. and isomer are comparable in  $^{235}\text{U}(n_{th},f)$  and  $^{238}\text{U}(600\text{ MeV } p,f)$ .

The fact that counting statistics is weaker than in the experiment by Becker *et al.* [3] may explain why the weakest among the reported transitions, namely, those with  $I_\gamma < 1$ , are not seen in this work. However, we have been able to detect

TABLE I. Transitions in the decay of  $^{98}\text{Rb}$  to  $^{98}\text{Sr}$ . Energies and intensities are obtained from singles and coincidences. Coincidence relationships are listed by merging data of both detectors except for  $E < 140$  keV (projection is onto planar Ge only), and  $E > 511$  keV (onto coaxial Ge only). Coincidences are within brackets if the ratio of peak area to its error is less than 3.

Energy (keV)		Intensity from			Placed to		Coincidences
71.0	(1)	2.1	(2)		216	145	145, 656, (1324)
107.2	(1)	2.1	(2)	<sup>a</sup>	2231	2124	145, (286), 523, 586, 656, (727), 1253, (1456), (1693), 1980
140.6	(1)	3.9	(3)		1978	1838	(107), 145, (289), 1693
144.5	(1)	100	-		145	0	107, 141, (145), (175), 286, 289, 433, 511, 631, 656, (668), 727, (810), 1080, (1093), 1106, (1253), (1324), (1360), 1456, (1601), 1693, 1772, (1778), 1820, (1926), (2086), (2094), 2145, 2172, (2498), (2660) 3009, 3029, 3146, (3478)
175.1	(2)	0.4	(1)	<sup>b</sup>	2154	1978	(141), (145), (1693)
192.1	(4)	0.5	(3)	<sup>b</sup>	(2316	2124)	(1693)
215.5	(1)	7.8	(9)	<sup>c</sup>	216	0	
234.2	(4)	0.8	(4)	<sup>b</sup>	(2359	2124)	(1693)
286.2	(2)	0.5	(1)	<sup>b</sup>	2124	1838	(107), (145)
289.3	(1)	32.6	(17)		434	145	145, 433, (511), 1105, 1772, (1926), (2498), 3009, 3029
433.2	(2)	1.5	(2)		867	434	145, 289
523.4	(3)	0.5	(2)	<sup>b</sup>	2124	1600	107
585.0	(3)	0.4	(2)	<sup>b</sup>	2124	1539	107
605.4	(2)	1.2	(2)	<sup>b</sup>	(2206	1600)	(1456)
630.7	(2)	3.0	(3)		2231	1600	(145), (1456)
655.8	(2)	8.4	(8)		871	216	71, 145
668.1	(3)	1.1	(2)	<sup>d</sup>	1539	871	(145)
726.8	(2)	1.9	(3)		871	145	145
810.4	(4)	0.3	(1)	<sup>b</sup>	1681	871	(71), (145), (656)
871.4	(3)	2.1	(3)		871	0	(107)
1079.7	(3)	2.2	(3)		1224	145	145
1092.8	(3)	2.0	(3)		1964	871	(71), 145, (656)
1105.5	(3)	1.7	(3)		1539	434	145, 289
1167.1	(4)	0.5	(2)	<sup>d</sup>	(1600	434)	(145)
1253.2	(4)	0.7	(2)	<sup>d</sup>	2124	871	(71), 107, (145)
1323.9	(3)	2.0	(4)	<sup>b</sup>	1539	216	(71), (145)
1359.8	(3)	3.0	(5)	<sup>d</sup>	2231	871	(145), (656)
1403.9	(4)	0.6	(2)	<sup>d</sup>	1838	434	(289)
1455.9	(3)	6.9	(5)		1600	145	(107), 145, (606), (631)
1539.2	(4)	0.8	(3)	<sup>b</sup>	1539	0	(107)
1600.4	(3)	1.7	(9)	<sup>e</sup>	(1600	0)	
1600.6	(4)	1.6	(4)	<sup>b</sup>	(1745	145)	(145)
1693.2	(2)	15.5	(13)		1838	145	(107), 140, 145, (175)
1772.0	(3)	3.5	(5)		2206	434	145, 289
1777.7	(4)	1.8	(3)		(1922	145)	(145)
1819.5	(3)	4.4	(4)		1964	145	145
1925.5	(4)	1.8	(3)	<sup>b</sup>	2359	434	(145), (289)
1964.1	(4)	2.4	(6)		(1964	0)	
1979.6	(3)	1.2	(3)	<sup>f</sup>	2124	145	107, (145)
2086.3	(4)	1.0	(3)		2231	145	(145)
2092.9	(4)	1.3	(3)	<sup>b</sup>	(2237	145)	(145)
2144.5	(3)	3.4	(5)	<sup>f</sup>	(2288	145)	145
2171.5	(3)	15.7	(15)		2316	145	145

TABLE I. (*Continued*).

Energy (keV)		Intensity from		Placed to		Coincidences
2214.7	(4)	0.8	(2)	<sup>b</sup>	2359	145 (145)
2315.8	(4)	7.5	(21)	<sup>g</sup>	(2316	0)
2498.2	(4)	1.7	(3)		2932	434 (145), (289)
2659.8	(4)	1.5	(3)	<sup>b</sup>	(2804	145) (145)
2804.2	(4)	2.1	(5)	<sup>g</sup>	(2804	0)
3008.6	(4)	7.0	(7)		3443	434 145, 289
3028.6	(4)	2.9	(5)		3463	434 145, (289)
3145.9	(5)	2.1	(4)		3290	145 145
3290.2	(6)	3.6	(14)	<sup>g</sup>	(3290	0)
3478.1	(6)	1.1	(3)		3623	145 (145)
3622.4	(7)	1.7	(7)	<sup>g</sup>	(3623	0)

<sup>a</sup>Line reported in Ref. [3] but not placed.

<sup>b</sup>New line observed in coincidence spectra.

<sup>c</sup>The intensity of this  $E0$  transition is calculated from Ref. [21].

<sup>d</sup>Partial coincidence data due to low statistics.

<sup>e</sup>From difference between intensity in singles and in gate on 145-keV transition.

<sup>f</sup>Line placed as a g.s. transition in Ref. [3].

<sup>g</sup>New line observed in singles spectra and placed by energy fitting only.

and place several new transitions with intensities lower than this limit. We also note that calculated energies above 3 MeV show substantial deviations with respect to the original values. Above 1.4 MeV the energy calibration for the present work was made internally using evaluated data for transitions in  $^{98}\text{Zr}$  [21].

Up to the 1600-keV level included, the new level scheme is in good agreement with the one presented by Becker *et al.* [3]. We assume, as in their work, that the 1224-keV level is a  $0^+$  state. At this low excitation energy, only  $0^+$  and  $2^+$  states can be expected in addition to the levels of the g.s. band. The absence of feeding transitions from any level (while all well-established  $2^+$  states are populated from higher-lying levels) as well as the missing g.s. transition seem unlikely in case of  $I=2$ .

The placement of a 1600-keV g.s. transition deserves a comment. A 1600-keV  $\gamma$  ray is observed in coincidence with the 144.5-keV  $2^+ \rightarrow 0^+$  transition. However, the intensity of the peak in the singles spectrum is higher than is calculated from the above coincidence. In agreement with Ref. [3], we therefore place the residual intensity as a 1600-keV g.s. transition. This placement is based on energy fitting only, since the overly weak intensity does not allow one to conclude about the existence of coincidence relationships with higher-lying lines.

A new level at 1682 keV is introduced by placing the 810 keV transition on top of the 871-keV level, according to its coincidences with the 71-, 145-, and 656-keV transitions. These are weak but form a consistent set.

The 1838-keV g.s. transition [3] is not confirmed. The 1980-keV  $\gamma$  ray, the next higher g.s. transition in Ref. [3], actually depopulates a new level at 2124 keV. These revisions are of consequence, since they release the 1838- and 1978-keV levels from the necessity of having  $I=(1,2)$ . A

new interpretation of these levels is discussed in the following section.

The new 2124-keV level shows a fragmented decay. It has decay branches to all well-established  $2^+$  levels, as well as to the probable  $2^+$  level at 1600 keV and the level at 1838 keV. The feedings from the 2231-keV level via the 107 keV transition and from levels at 2316 and 2358 keV, which are  $I=(1,2)$  states, do not let room for direct population in  $\beta$  decay. These links and the absence of branches to  $0^+$  or  $4^+$  states are logical if  $I^\pi=2^-$  is assumed, which we therefore propose tentatively, although  $I=1$  and 3 cannot be ruled out. The gate on the 107-keV transition (see Fig. 2) shows the depopulation of this new level.

The 2145-keV level postulated in Ref. [3] is not confirmed. The g.s. transition has to be placed elsewhere due to its coincidence with the 145-keV transition, while the reported weak 2000-keV transition is not seen at all. Moreover, it is probable that the 167-keV transition seen in the 140-keV gate is entirely due to the coincidence of the strong lines of 141 and 167 keV in  $^{97}\text{Sr}$ , which is populated in  $\beta$ -delayed neutron decay of  $^{98}\text{Rb}$ .

The 2231-keV level is strongly fed in  $\beta$  decay. The intensity balance of the 2124-keV level favors the lowest possible conversion of the 107-keV transition. If of  $M1$  character, the 107-keV transition could be a hint for a  $K=2$  band formed by the 2124- and 2231-keV levels. However, there is no suitable candidate for the next band member with  $I=4$ . Thus this feature could be accidental.

Centroid shifts of time distributions with gates on high-energy transitions in the larger Ge detector do not reveal any significant shift outside the scattering of data within a typical 1-ns band, except for the already reported 1693-keV transition with  $t_{1/2}=7.1(8)$  ns, assigned to the 1838-keV level [18]. A centroid plot is shown in Fig. 3. The delayed coinci-

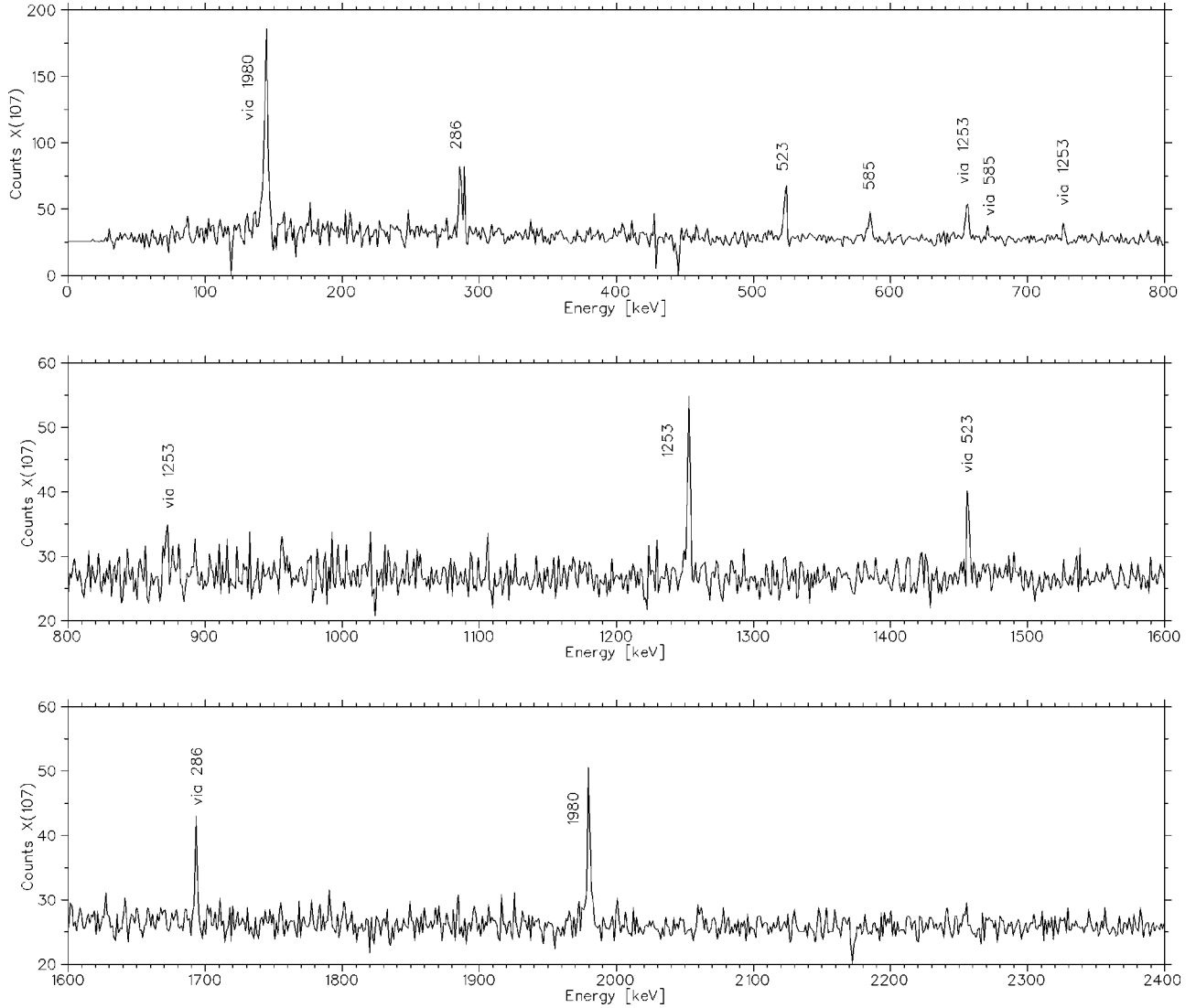


FIG. 2. Gate on the 107-keV transition showing the decay of the 2124-keV level. Transitions leaving the 2124-keV level and the strongest ones of the next generation are marked. The 144-keV  $2^+ \rightarrow 0^+$  transition collects all of the intensity except for a small fraction flowing via the  $E0$  transition from the 216-keV level.

dences with gates on low-energy transitions in the planar detector qualitatively confirm a measurable lifetime for the 1838-keV level. However, the spectrum gated by the 140-keV transition above the isomer is difficult to exploit due to interference of the 141-keV line in  $^{97}\text{Sr}$ . There is no measurable lifetime for the new 2124-keV level, as shown by the spectrum gated by the 107-keV transition. The relevant time spectra are shown in Fig. 4. For the analysis of the 216-keV  $0^+$  level, a gate was set on the 71-keV transition. The slope method yielded a somewhat smaller result than reported in Ref. [24] [ $t_{1/2} = 25(2)$  ns], namely, 21.2(17) ns.

#### 1. A band on the 7.1-ns isomeric level at 1838 keV

The 1838-keV level decays to the  $2_1^+$  state via the 1693-keV transition and to the  $4^+$  state by a weaker branch. Thus, the spin could be  $I=3$  or 4 as alternatives to the former  $2^+$  assignment based on the incorrectly placed g.s. transition. Becker *et al.* [3] showed that their angular-correlation coef-

ficients for the 1693–145-keV cascade [ $A_{22} = -0.25(15)$  and  $A_{44} = 0.49(28)$ ] are consistent with  $I=2$ . Nevertheless,  $I=3$  cannot be rejected. There are solutions for  $A_{22}(\delta_{1693})$ , one with a small  $E2$  admixture consistent with zero and another one with a very large  $E2$  component. For both  $I=2$  and 3, the small  $\delta$  value gives a better agreement for  $A_{44}$ , but still the agreement is poor.

The 1838-keV level has a half-life of 7.1 ns. Hindrances for the transitions to the  $2^+$  and  $4^+$  states of the g.s. band are shown for the possible multipolarities in Table II. The hindrances per degree of forbiddenness are unusually high for  $K=2$  and still remain high for  $K=3$ . Even parity gives the lowest hindrances, in better agreement with local systematics. This parity is also favored by logft values, as is discussed in Sec. IV.

The 140-keV and new 175-keV transitions form a cascade on top of the 1838-keV level. The energies suggest a rotational band. The ratio of energies  $(E_{K+2} - E_{K+1}) / (E_{K+1} - E_K)$



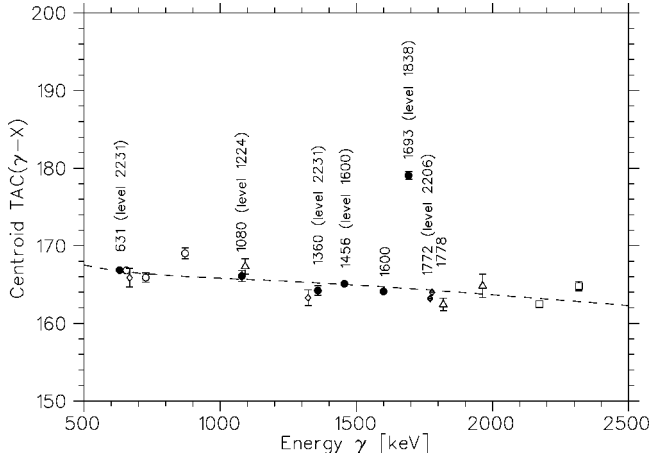


FIG. 3. Centroid-shift plot from  $\gamma$ - $\gamma$ - $t$  coincidences for some high-energy lines in  $^{98}\text{Sr}$ ; see the text for details. The scattering of the points gives an indication of systematical errors. The prompt curve (dashed line) is obtained by an eye-guided interpolation using numerous transitions in the  $A=98$  and  $97$  mass chains. The conversion is  $0.68$  ns/channel. The centroid of the  $1693$ -keV gated spectrum is the only one with a definite shift. Open circles, diamonds, triangles, and squares refer to lines from the  $871$ -,  $1539$ -,  $1964$ -, and  $2316$ -keV levels, respectively. Closed circles indicate transitions from levels discussed in the text.

TABLE II. Hindrances for transitions depopulating the  $1838$ -keV level in  $^{98}\text{Sr}$  ( $t_{1/2}=7.1$  ns) to  $2^+$  ( $1693$  keV  $\gamma$ -ray) and  $4^+$  ( $1404$  keV  $\gamma$ -ray) states of the g.s. band. The  $K$  values of  $2$  and  $3$  are those allowed by angular correlation data [3]. The hindrance per degree of forbiddenness  $h$  is defined by  $H=h^n$ , where the hindrance  $H$  is the ratio of the experimental partial half life to the Weisskopf estimate and  $n=|\Delta K|-L$ .

$I^\pi$	Transition	$ML$	W.u.	$H$	$n$	$h$
$2^+$	1693	$M1$	$4.6 \times 10^{-12}$	$1.6 \times 10^6$	1	$1.6 \times 10^6$
	1404	$E2$	$3.8 \times 10^{-12}$	$5.0 \times 10^4$	0	
$2^-$	1693	$E1$	$6.7 \times 10^{-17}$	$1.1 \times 10^8$	1	$1.1 \times 10^8$
	1404	$M2$	$2.7 \times 10^{-10}$	$7.0 \times 10^2$	0	
$3^+$	1693	$M1$	$4.6 \times 10^{-12}$	$1.6 \times 10^6$	2	$1.2 \times 10^3$
	1404	$M1$	$8.1 \times 10^{-15}$	$2.4 \times 10^7$	2	$4.8 \times 10^3$
$3^-$	1693	$E1$	$6.7 \times 10^{-17}$	$1.1 \times 10^8$	2	$1.0 \times 10^4$
	1404	$E1$	$1.2 \times 10^{-16}$	$1.6 \times 10^9$	2	$4.0 \times 10^4$

$-E_K$ ) agrees perfectly with the rotational spacings for  $K=3$ . A tentative coincidence in the  $1693$ -keV gate (see Fig. 5) could represent the next  $6 \rightarrow 5$  transition of  $210.8(5)$  keV with an intensity of about  $0.2$  relative units. A further test is the distribution of  $\beta$ -feeding intensities among the assumed band members. The levels of interest are expected to be populated by the high-spin  $^{98}\text{Rb}$  decay only, since the low-

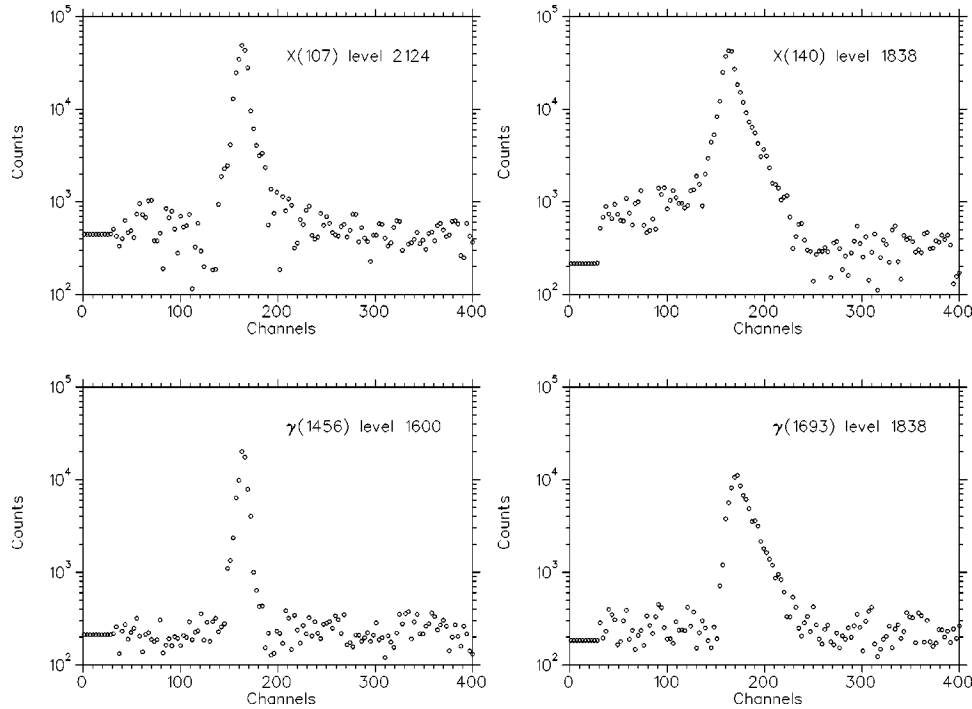


FIG. 4. Delayed-coincidence spectra for the  $107$ - and  $140$ -keV lines gated with the planar detector, and  $1456$ - and  $1693$ -keV lines gated in the coaxial detector. The  $x$  axis is in channels with a conversion of  $0.68$  ns/channel. For better clarity, counts have been averaged on three neighboring channels, and each third channel is plotted. A constant has been added in order to avoid display of negative counts. No lifetime is visible for the  $107$ -keV line, showing that the  $2124$ -keV level is short lived. The small tail on the right-hand side of the peak is due to the link of the  $2124$ -keV level to the isomer at  $1838$  keV. The slopes observed for the  $140$ - and  $1693$ -keV gated spectra show that the lifetime is due to the  $1838$ -keV level. Contamination by the  $141$ -keV line in  $^{97}\text{Sr}$  is responsible for the tail on the left-hand side of the spectrum of the  $140$ -keV line. The  $7.1(8)$ -ns half life is deduced from the slope of the spectrum gated by the  $1693$ -keV transition. The  $1456$ -keV line gives an indication of the timing response.

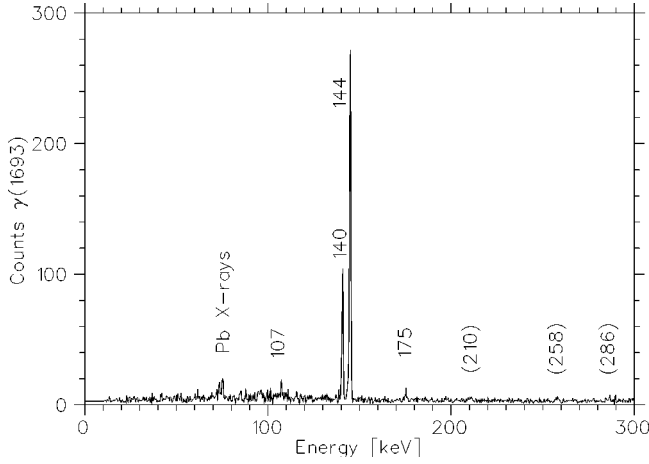


FIG. 5. Gate on the 1693-keV transition showing the 140- and 175-keV transitions forming the proposed  $5 \rightarrow 4 \rightarrow 3$  cascade. The very weak peak at 210 keV could be due to the next  $6 \rightarrow 5$  transition. The other very weak line at 258 keV has not been placed. The coincidence with the 107-keV transition occurs via the intermediate 286-keV line from the 2124-keV level.

spin level has  $I=(0,1)$  according to Ref. [21]. The relative experimental  $\beta$  feedings of the 1838- (0.73) and 1979-keV (0.25) levels indeed are in satisfactory agreement with the Alaga rule for both  $I(^{98}\text{Rb})=3$  or 4 if  $K=3$ . We note that the weak  $\beta$  feeding of the 2154-keV level (0.02) could easily be cancelled in the case of additional feeding by non detected  $\gamma$  transitions. Accordingly, it would be premature to conclude  $I=4$  for  $^{98}\text{Rb}$ .

Based on the above discussion, we propose the 1838-keV level to be a  $K=3$  band head of probable even parity. The 1979- and new 2154-keV levels are  $K+1$  and  $K+2$  band members.

## 2. Decay of $^{98}\text{Rb}$

The strong feeding to the  $K=3$  level at 1838 keV is not consistent with  $I=5$  for the  $^{98}\text{Rb}$  high-spin level, as stated in Ref. [21]. Instead,  $I=3$  and 4 with both parities have to be considered. We present a decomposition of  $\beta$ -feeding intensities for  $I=3$  in Table III. This is only one among several possibilities, and a few arbitrary assumptions still need to be made. Nevertheless, it is instructive for a discussion of  $\beta$ -feeding patterns. In this particular case, the feedings to high-lying levels with  $I=(1,2)$  and of unplaced transitions have been evenly shared among the low- and high-spin decays, while feeding of  $2^+$  states was regarded as negligible in the low-spin decay. The  $\log ft$  value of 5.7 for the 216-keV  $0^+$  level could indicate an allowed transition and  $I(\text{Rb})=1^+$ . It varies by 0.3 units when removing or adding the shared intensity. Moreover, it must rise if the ground state and some  $2^+$  states are  $\beta$  fed. There are conflicting measurements of the g.s. branching [22,23]. Thus it is not possible to unambiguously assign a parity for the low-spin Rb level. The  $\log ft$  values for the high-spin decay are less sensitive to the unplaced intensity. The  $\log ft$  values for the  $2^+$  levels, the 434-keV  $4^+$  state of the g.s. band, and for the  $K=3$  isomer, are slightly below 5.9. The values for transitions to  $2^+$  states

TABLE III. Beta feedings and  $\log ft$  values if  $I(^{98}\text{Rb}, 116 \text{ ms})=(0,1)$  and  $I(^{98}\text{Rb}, 96 \text{ ms})=3$  under further assumptions described in the text. If no entry, direct  $\beta$  feeding has been assumed to be neglectable.  $\log ft$  values are calculated with  $Q_\beta=12.3 \text{ MeV}$  [21].

Level	$I^\pi$	$\beta$ feeding $I=(0,1)$	$\log(ft)$	$\beta$ feeding $I=3$	$\log(ft)$
0.0	$0^+$				
144.5	(1) $2^+$			16.4 (20)	5.7
215.5	(1) $0^+$	20.7 (17)	5.7		
433.9	(2) $4^+$			9.6 (15)	5.8
867.2	(2) $6^+$			1.3 (2)	6.7
871.4	(1) $2^+$			5.2 (9)	6.0
1224.2	(3) $(0^+)^a$	6.2 (9)	6.0		
1539.4	(2) $2^+$			4.4 (5)	6.0
1600.4	(2) $(2^+)$			4.6 (7)	6.0
1681.8	(4) $(4^+)^b$			0.3 (1)	7.1
1837.8	(2) $(3^+)^c$			9.4 (11)	5.6
1964.1	(2) $(1,2)^d$	12.6 (12)	5.6	3.7 (4)	6.0
1978.4	(3) $(4^+)$			3.2 (3)	6.1
2124.1	(2) $(2^-)^e$			-0.1 (6)	
2153.5	(3) $(5^+)$			0.3 (1)	7.1
2205.9	(2)			4.0 (4)	5.9
2231.2	(2) $(2,3)^f$			7.9 (6)	5.5
2316.0	(2) $(1,2)^d$	34.1 (23)	5.1	9.8 (7)	5.5
2358.9	(4)			2.9 (5)	6.0
2804.4	(4) $(1,2)^d$	4.5 (9)	5.6	1.5 (3)	6.2
2931.8	(4)			1.4 (3)	6.2
3290.3	(4) $(1,2)^d$	7.8 (19)	5.5	2.4 (6)	5.9
3442.5	(4)			5.9 (5)	5.5
3462.5	(4)			2.5 (3)	5.9
3622.6	(5) $(1,2)^d$	4.0 (9)	5.8	1.2 (3)	6.2

<sup>a</sup> $I^\pi=0^+$  is tentatively assumed due to the absence of transitions and for structural reasons.

<sup>b</sup>Tentative spin assignment assuming a two-phonon level.

<sup>c</sup> $K$  isomer assigned in this work from band structure and hindrances.

<sup>d</sup>Half of the experimental  $\beta$  feeding has been shared between high- and low-spin decays.

<sup>e</sup>Assignment based on calculated quasi-particle structure; see the text. Feeding is calculated with  $E1$  multipolarity for the 107-keV transition.

<sup>f</sup> $I^\pi=3^+$  favored by absence of transitions to  $0^+$  states, a large branching ratio of the transition to the assumed  $2^-$  state at 2124 keV, and a strong population in  $\beta$  decay.

could be higher if part of feedings to  $2^+$  states is moved to the low-spin decay. This, however, would lower the  $\log ft$  values for the decays to the  $4^+$  and  $K=3$  levels. Therefore, allowed character for these transitions is more probable than first forbidden. We note that the relative  $\beta$  feedings of the 2124- and 2231-keV levels are not in accordance with  $I(^{98}\text{Rb})=3$  if these levels would belong to a  $K=2$  band.

The other choice of  $I=4$  for  $^{98}\text{Rb}$  allows a decomposition with less arbitrary assumptions. The  $2^+$  levels must then be fed in the low-spin decay. This leads to  $I=1$  for the low-spin  $^{98}\text{Rb}$  level but, still, the parity is not determined. In the high-

spin decay the  $\log ft$  values to the  $K=3$  and  $4^+$  states are lowered by 0.2–0.3 units with respect to the values in Table III. They remain in the range of allowed transitions even when fully adding the contributions of nonplaced intensity.

In conclusion, it is not possible to assign spin and parity for the low-spin level in  $^{98}\text{Rb}$ . For the higher-spin level, even parity is favored for  $I=3$  and appears probable for  $I=4$ . In either case of  $I(^{98}\text{Rb})=3$  or 4, the  $\log ft$  value for  $\beta$  decay to the 1838-keV level is slightly below the limit for first-forbidden transitions. Thus, the even parity of the  $K=3$  band head, in agreement with arguments of hindrances mentioned earlier, is the most probable.

### B. New levels in $^{100}\text{Zr}$

New transitions are established by coincidence relationships to belong to the level scheme of  $^{100}\text{Zr}$ ; see Table IV. We assume that they belong to the decay of the high-spin isomer, based on the argument that it is unlikely that these fairly strong transitions would have escaped detection in the decay study of the low-spin  $^{100}\text{Y}$  performed with superior statistics at TRISTAN [4,7]. The intensities of the new transitions are calculated from the number of coincidences. For those transitions also reported in the low-spin decay of  $^{100}\text{Y}$ , a correction is made. The contribution to be subtracted is defined under the assumption that the high-lying  $I=(1,2)$  levels are not significantly fed in the high-spin decay. The strongest direct  $\beta$  feeding is the one to the  $4^+$  state of the g.s. band; see Table V. The feedings to the first excited  $2^+$  and two other  $2^+$  states are sizable, but are largely dependent on the corrections. It might therefore be premature to conclude that  $I=3$  for  $^{100}\text{Y}$ . We do not observe any enhancement of the population with respect to the low-spin decay of  $^{100}\text{Y}$ , nor any link with the new levels for the 829-keV  $0^+$  state and the 1295-keV level. This indicates a low spin for the 1295-keV level.

The 1441-keV  $2^+$  level was observed previously in  $\beta$  decay. The intensities of the 1229- and 1110-keV transitions, when calculated in the 213- and 119-keV gates, agree with the values of Ref. [4], but are different when gating on the new 907-keV transition feeding the 1441-keV level. This suggests the 1229-keV line to be a doublet. However, the second component could not be placed.

The 1414- and 1856-keV levels were reported in two prompt-fission experiments in the deexcitation of the band head at 2260 keV [9–11]. In Ref. [10] the authors extended the band on the excited  $0^+$  state at 331 keV by assigning them as the  $4^+$  and  $6^+$  band members. We cannot conclude about transitions from the 1414-keV level to  $2^+$  states as stated in that work. The 535-keV transition is masked by the residual of the very strong  $2^+ \rightarrow 0^+$  transition in  $^{100}\text{Mo}$ , and the other 1201-keV transition is presumably too weak to be observed in our data.

The absence of any signature for a  $3^+$  state as corresponding to the 1838-keV level in  $^{98}\text{Sr}$  is a surprise. We failed to observe a level with a measurable lifetime (beyond the ns), or a state with a cascade of suitable low-energy transitions on top of it. It is difficult to understand why no level with  $I=3, 4$ , or 5 of the expected band could be iden-

tified, while the  $4^+$  state of the g.s. band is rather strongly fed. It might be worth noting that a similar situation might occur as in the  $N=59$  isotones  $^{97}\text{Sr}$  and  $^{99}\text{Zr}$ . A well developed  $K^\pi=3/2^+$  band has been observed in the former [9], but could not be identified so far in the latter [2].

## C. Theoretical description of the two-quasiparticle levels in $^{98}\text{Sr}$

### 1. Ground-state deformations and single-particle levels

Equilibrium deformations and moments, potential-energy surfaces, microscopic structure of coexisting configurations, and shape-transitions in the heavy Sr-Zr region have been calculated by several authors [25–28]. Recently, the deformed shell model combined with the quantum Monte Carlo method for pairing calculations was employed to study the two-quasineutron level structure in the  $A \approx 100$  region [16]. The same theoretical formalism is used in the present work. The average field was assumed to be an axially deformed Woods-Saxon potential [29] with a cassinian oval shape parametrization [30]. The universal Woods-Saxon parameters were those proposed by Dudek and co-workers [31,32], except for smaller values of the central potential radius parameter ( $R_{0C}=1.25$  and 1.32 fm for proton and neutron systems, respectively, following Ref. [33]). The radius of the neutron potential is larger than the 1.25 fm previously employed in Ref. [16]. It reflects the experimental difference between neutron and proton matter distributions. However, this modification has hardly any noticeable influence on the calculated deformation energy surface.

The  $^{98}\text{Sr}$  and  $^{100}\text{Zr}$  isotones are predicted to have well-deformed prolate ground states with calculated Cassinian deformations  $\epsilon$  ranging from approximately 0.30 to 0.36, i.e.,  $\beta_2$  values from 0.32 to 0.40. These values were also found in previous theoretical studies [27,28] and are in good agreement with experimental deformations [5–7]. Figures 6 and 7 show Nilsson diagrams calculated with our Wood-Saxon potential parameters for neutrons and protons near the Fermi levels in this region. It is worth mentioning the 2-MeV gap obtained between  $\pi[431]3/2$  and  $\pi[422]5/2$  orbitals in the proton system. These configurations become Fermi levels in  $^{98}\text{Sr}$  ( $Z=38$ ) and  $^{100}\text{Zr}$  ( $Z=40$ ), respectively. This large energy gap results in quite different excitation energies of two-quasiproton states in  $^{98}\text{Sr}$  and  $^{100}\text{Zr}$ . The lowest two-quasiparticle (2QP) excited levels in  $^{98}\text{Sr}$  will certainly originate from the neutron system. However, the situation could be different for  $^{100}\text{Zr}$  in which a proton pair is above the  $Z=38$  gap. Single-particle energies for  $^{98}\text{Sr}$ , calculated at the experimental g.s. equilibrium deformation, are presented in Table VI.

### 2. Pairing calculation

The excitation energy of a two-quasiparticle band is determined, neglecting the Gallagher spin-spin shift of the two-quasiparticle states [34], by the strength  $G$  of the pairing interaction and the energies of the contributing single-particle states relative to the Fermi level. We extracted the experimental pairing energy from nuclear masses according to the prescription in Ref. [35]. Theoretical pairing energies



TABLE IV. Transitions placed in  $^{100}\text{Zr}$  and so far not reported in  $\beta$  decay of  $^{100}\text{Y}$  or of stronger population than in the  $\beta$  decay study of Ref. [4] and transitions in subsequent decays. Coincidences are listed with the new transitions only, since the data are symmetric with exchange of gates and projections.

Energy (keV)		Intensity from		Placed to		Coincidences	
118.6	(2)	28.5	(63)		331	213	
212.5	(1)	322.	(58)		213	0	
314.0		0.4	(2)	<sup>a</sup>	879	564	
318.0		0.8	(4)	<sup>a</sup>	1196	879	
331.1	(2)	13.6	(53)	<sup>b</sup>	331	0	
351.8	(2)	100	(8)		564	213	
353.0		0.6	(2)	<sup>c</sup>	1414	1061	
497.1	(2)	6.2	(6)	<sup>d</sup>	1061	564	213, 352, (900)
547.4	(2)	14.7	(23)		879	331	
631.6	(2)	3.8	(8)		1196	564	
665.8	(2)	40.2	(55)		879	213	
672.4	(2)	7.0	(12)	<sup>e</sup>	2070	1398	213, 352, 1185
833.5	(3)	2.8	(10)	<sup>e</sup>	1398	564	213, 352
850.1	(3)	9.3	(8)	<sup>f</sup>	1414	564	213, 352
865.0	(2)	14.2	(23)		1196	331	
874.3	(3)	8.7	(17)	<sup>e</sup>	2070	1196	119, 213, 352, 1196
878.6	(2)	22.5	(34)		879	0	
900.1	(3)	1.1	(4)	<sup>g</sup>	1962	1061	(213), 352, (497)
907.8	(3)	13.8	(16)	<sup>e</sup>	2349	1441	119, 213, 1110, 1229, 1441
983.2	(3)	7.0	(12)		1196	213	
1110.1	(3)	4.3	(8)		1441	331	
1153.0	(3)	11.1	(15)	<sup>e</sup>	2349	1196	119, 213, 352, 632, 865, 1196
1185.4	(3)	17.7	(15)	<sup>e</sup>	1398	213	213, 672
1191.6	(3)	22.1	(17)	<sup>e</sup>	2070	879	119, 213, 666, 879
1196.2	(2)	20.4	(27)		1196	0	
1229.0	(3)	4.9	(10)		1441	213	213, 908
1291.5	(3)	4.2	(6)	<sup>f</sup>	1856	564	213, 352
1438.6	(4)	3.4	(8)	<sup>e</sup>	(2002)	564)	(213), 352
1441.4	(2)	3.6	(6)		1441	0	
1471.0	(3)	27.4	(27)	<sup>e</sup>	2349	879	119, 213, 547, 666, 879
1505.5	(5)	3.0	(8)	<sup>e</sup>	2070	564	213, 352
1644.2	(3)	3.2	(8)	<sup>h</sup>			213
1655.8	(3)	5.9	(10)	<sup>e</sup>	2220	564	213, 352
1857.8	(4)	7.7	(21)	<sup>e</sup>	2070	213	213
2008.0	(8)	1.3	(8)	<sup>e</sup>	(2220)	213)	(213)
2137.0	(8)	4.3	(17)	<sup>e</sup>	2349	213	(213)

<sup>a</sup>Intensity calculated from Ref. [7], since the transition is too weak to be seen here.

<sup>b</sup>The intensity of this  $E0$  transition is calculated from Ref. [21].

<sup>c</sup>Line reported in Ref. [11]. In this work, this line is supported by the presence of a peak at 352 keV in the gate of same energy.

<sup>d</sup> $6^+ \rightarrow 4^+$  transition in the g.s. band [9–11].

<sup>e</sup>New transition in  $\beta$  decay of  $^{100}\text{Y}$ .

<sup>f</sup>Reported in Refs. [9–11].

<sup>g</sup>Reported in Refs. [9,10].

<sup>h</sup>Possibly not from the 1856-keV level reported in prompt fission [9–11], since there is a poor level energy fitting and the transition was not reported in these works.

were computed using the Lipkin-Nogami (LN) method [36]. All single-particle orbitals in a 16 MeV interval around the Fermi energy were included in the calculations. The monopole pairing strength was adjusted to reproduce experimental

pairing energies. Using the obtained pairing strength, we calculated the solution for the pairing problem using both quantum Monte Carlo (QMC) [16,37] and Monte Carlo projection (MCP) methods [38]. In the latter case, the projection started

TABLE V. Levels of  $^{100}\text{Zr}$  populated by the high-spin level of  $^{100}\text{Y}$ . The  $\log ft$  values are calculated with  $Q_\beta=9.31$  MeV and  $T_{1/2}=0.94$  s [21].

Energy	$\beta$ feeding	$\log(ft)$	$I^\pi$
0.0	0.		$0^+$
212.5	(1) 28.1 (111)	5.9	$2^+$ <sup>a</sup>
331.1	(2) 2.3 (23)	6.9	$0^+$
564.3	(2) 16.9 (32)	6.0	$4^+$ <sup>a</sup>
878.5	(2) 7.2 (22)	6.3	$2^+$
1061.4	(3) 1.6 (3)	6.9	$6^+$ <sup>a</sup>
1196.0	(2) 6.9 (15)	6.3	$2^+$
1397.9	(3) 3.6 (8)	6.5	<sup>b</sup>
1414.4	(4) 2.4 (5)	6.7	$(4^+)$ <sup>c</sup>
1441.4	(2) -0.3 (6)		$2^+$
1856.3	(5) 1.9 (4)	6.7	$(6^+)$ <sup>c</sup>
1961.5	(5) 0.5 (2)	7.3	<sup>d</sup>
2070.2	(2) 12.7 (22)	5.8	<sup>b</sup>
2220.1	(4) 1.9 (5)	6.6	<sup>b</sup>
2349.3	(2) 14.8 (25)	5.7	<sup>b</sup>

<sup>a</sup>Belongs to the g.s. band [9–11].

<sup>b</sup>New level.

<sup>c</sup>Observed in the depopulation of a  $5^-$  or  $6^+$  band head in prompt fission [9–11].

<sup>d</sup>Belongs to a side band [9,10].

from the obtained Lipkin-Nogami solution. Both Monte Carlo methods are exact within the statistical uncertainty of the Monte Carlo calculation [16,38].

We have calculated ground-state  $\Delta E_{GS}(G)$  and two-quasiparticle  $\Delta E_{2QP}(G)$  pairing energies for  $^{98}\text{Sr}$ . In this case, the single-particle level densities are rather low. It is therefore essential to take into account the blocking effect of the unpaired nucleons. Thus, for a two-quasiparticle state calculation, the particle number  $N$  is accordingly reduced by two and the blocked states are removed. Results of the LN, QMC, and MCP calculations are shown in Table VII. The excellent agreement between QMC and MCP methods gives

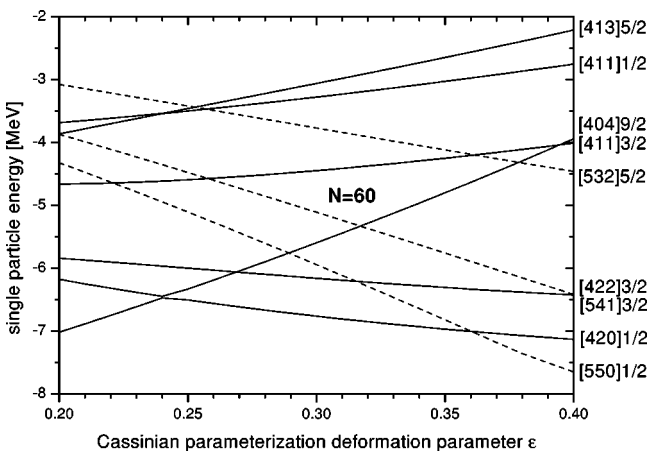


FIG. 6. Expanded portion of the Nilsson diagram for neutrons in the  $N=60$  region. The energies were calculated using the Woods-Saxon potential parameters described in the text.

confidence in the accuracy of Monte Carlo pairing calculations. It is interesting to point out that the Monte Carlo and LN methods give similar results. For energy bandhead calculations, MCP results were selected, considering they have smaller uncertainties than QMC calculations.

## IV. DISCUSSION

### A. Low-lying levels

The  $^{98}\text{Sr}$  ground state, together with that of  $^{100}\text{Sr}$ , is the most deformed one in the  $A \approx 100$  region with  $\beta=0.40$  [5,6,19] while  $^{100}\text{Zr}$  is only slightly less deformed with  $\beta=0.36$  [7]. The g.s. band of  $^{98}\text{Sr}$ , in particular, exhibits excellent rotational properties with a large and rigid moment of inertia [9,19]. According to the picture of shape coexistence and the transition taking place from  $N=58$  to 60, the  $0^+$  state at 216 keV corresponds to a very slightly deformed or even a spherical shape that could be associated with the g.s. of  $^{96}\text{Sr}$ . The 871-keV  $2^+$  level was proposed as the first phonon vibration of the spherical levels [3] but also as the head of the deformed  $\gamma$ -band [39]. Mixing of the closely lying  $0^+$  states makes transitions possible to both the g.s. and the excited  $0^+$  state. Spherical interpretation of the 871 keV level is supported by the strong preference for decay to the excited  $0_s^+$  state at 216 keV with  $B(E2,2 \rightarrow 0_s)/B(E2,2 \rightarrow 0_d) = 16.6$ . The corresponding  $2^+$  state in  $^{100}\text{Zr}$  is at 878 keV. These low-lying levels were presented as such in a review article on shape coexistence by Wood *et al.* [8].

Limited by the small number of definite spin assignments, one may attempt to use systematics of level energies and  $\gamma$ -branching patterns to identify further levels in  $^{98}\text{Sr}$ . The systematics of  $N=60$  isotones shows a rather smooth variation with proton number down to Mo ( $Z=42$ ). Unfortunately, the levels in  $^{100}\text{Zr}$  and  $^{98}\text{Sr}$  do not obviously correspond with those in their higher- $Z$  isotones. Therefore, we will search for analogies, comparing with the immediate neighbors of  $^{98}\text{Sr}$ , the spherical nucleus  $^{96}\text{Sr}$  [2,9,21] and the deformed, more neutron-rich, isotope  $^{100}\text{Sr}$  [40].

Spherical character looks probable for the  $2^+$  state at 1539 keV based on its strong branch to the 871-keV level and its preference to decay to the excited  $0^+$  state rather than to the ground state, e.g.,  $B(E2,2 \rightarrow 0_s)/B(E2,2 \rightarrow 0_d) = 5.3$ . A correspondance with the 1507-keV level in  $^{96}\text{Sr}$  looks quite reasonable. One can tentatively extend the comparison by including the 1224-keV level, by analogy with the  $0_2^+$  state at 1229 keV in  $^{96}\text{Sr}$ , into the set of spherical levels. The new level at 1682 keV in  $^{98}\text{Sr}$  could be the  $4^+$  spherical level based on a two-phonon excitation. The 810-keV transition, which is the only observed decay mode, is appealing as the two-to-one phonon transition. The assumed  $E_4/E_2$  ratio of  $1467/656 = 2.24$  compares very well with its value of 2.20 in  $^{96}\text{Sr}$ .

On the basis of these analogies with levels in  $^{96}\text{Sr}$ , the three levels at 1224, 1539, and 1682 keV form a possible ( $0^+$ ,  $2^+$ ,  $4^+$ ) triplet of spherical states. The low energies of the  $0^+$  and  $2^+$  states exclude a purely vibrational character.

TABLE VI. Single-particle levels close to the Fermi level for  $^{98}\text{Sr}$ , calculated using the Woods-Saxon potential at the experimental deformation of  $\beta_2=0.40$  ( $\epsilon=0.35$ ). The Fermi level is at the  $\nu[404]9/2$  and  $\pi[431]3/2$  orbitals.

Neutrons		Protons	
Orbital	Energy (MeV)	Orbital	Energy (MeV)
$\nu[422]3/2$	-6.28	$\pi[310]1/2$	-14.70
$\nu[541]5/2$	-5.63	$\pi[312]3/2$	-14.54
$\nu[404]9/2$	-4.96	$\pi[431]3/2$	-14.38
$\nu[411]3/2$	-4.29	$\pi[422]5/2$	-12.12
$\nu[532]5/2$	-4.05	$\pi[431]1/2$	-11.01
$\nu[411]1/2$	-3.08	$\pi[301]1/2$	-10.19

Such low-lying excited states have been reported in several near closed-shell regions where there exists a large gap for one type of nucleon. This is the case for  $^{96}\text{Sr}$  and the other  $N=58$  spherical isotones  $^{98}\text{Zr}$  and  $^{100}\text{Mo}$  [8]. These states have been interpreted as two-particle-two-hole excitations across the proton subshell gap [41]. The existence of depressed  $0^+$  and  $2^+$  states in  $^{98}\text{Sr}$  implies that the  $Z=40$  spherical subshell gap remains effective in spite of the presence of a coexisting strongly deformed minimum. This interpretation obviously deserves further investigation to be confirmed or not.

In contrast to above discussed levels, the 1600-keV level decays only to the g.s. band, with a strong preference for the  $2_1^+$  state. This favors the deformed interpretation and indicates a possible analogy with the 1315 keV level in  $^{100}\text{Sr}$ . Searching for a  $\gamma$  band, one notices the tentative levels at 1745 and 1922 keV which could be suitable as  $I=3$  and 4 band members. It would be very interesting to investigate this issue using prompt fission. The systematics of spherical and deformed states in  $^{98}\text{Sr}$ , as proposed in the above discussion, together with the corresponding levels in the  $^{96}\text{Sr}$  and  $^{100}\text{Sr}$  neighbors, is shown in Fig. 8.

TABLE VII. Quantum Monte Carlo, Monte Carlo projected, and Lipkin-Nogami pairing results for the pairing energies and two-quasi-neutron band-head energies (MeV) for a neutron pairing strength of  $G_N = 18.62/A$ . The statistical uncertainty of the QMC and MCP calculations are 0.2–0.3 and 0.1 MeV, respectively. The two-quasiparticle energies are given by  $U_{2QP} = U_{2P} + \Delta E_{GS}(G) - \Delta E_{2QP}(G)$ , where  $U_{2P}$  is the Fermi gas excitation energy,  $\Delta E_{GS}(G)$  and  $\Delta E_{2QP}(G)$  are pairing energies of ground state and of the two quasiparticle configurations. The g.s. values are  $\Delta E_{GS}(G) = 4.7, 4.5$  and  $4.61$  for QMC, MCP, and LN calculations, respectively. The values in column 6 are calculated with the MCP values of  $\Delta E_{GS}(G)$  and  $\Delta E_{2QP}(G)$ .

Configuration	$U_{2P}$	$\Delta E_{2QP}(G)$			$U_{2QP}$	Experimental
		QMC	MCP	LN		
$\nu[404]9/2 \otimes \nu[411]3/2$	0.67	3.4	3.4	3.03	1.77	$3^+$
$\nu[404]9/2 \otimes \nu[532]5/2$	0.91	3.3	3.3	3.10	2.11	$(2^-)$
$\nu[541]3/2 \otimes \nu[411]3/2$	1.34	3.4	3.3	3.30	2.49	
$\nu[541]3/2 \otimes \nu[532]5/2$	1.58	3.6	3.5	3.45	2.58	
$\nu[422]3/2 \otimes \nu[411]3/2$	1.99	3.5	3.4	3.40	3.09	<sup>a</sup>
$\nu[422]3/2 \otimes \nu[532]5/2$	2.23	3.7	3.5	3.52	3.23	

<sup>a</sup>The 2231-keV level is possibly the second  $3^+$  state but is quite low with respect to the calculation.

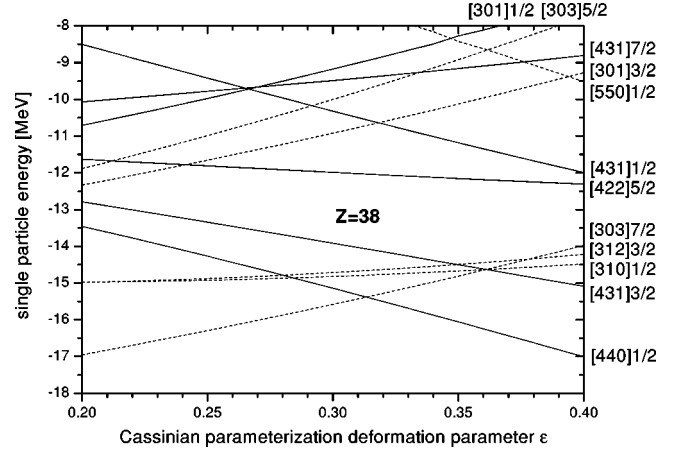


FIG. 7. Expanded portion of the Nilsson diagram for protons in the  $Z=40$  region. The energies were calculated using the Woods-Saxon potential parameters described in the text.

## B. QP levels

The  $I^\pi = 3^+ 1838$  keV level is an isomer due to the very large retardation of the transitions to the g.s. band, which is so far the largest observed in the  $A \approx 100$  region (Table VIII). The transitions of 175 and 140 keV form a  $5 \rightarrow 4 \rightarrow 3$  cascade, possibly extended by a 210-keV line. The moment of inertia, although very large with 87% of the rigid-rotor value, is lower than those of most other two-quasiparticle bands known in this region (Table IX).

As a consequence of the deformed  $Z=38$  gap, the lowest-lying quasiparticles in  $^{98}\text{Sr}$  are due to neutron excitations. The calculated sequence and level spacings are in good agreement with the data for odd- $N$  nuclei with  $N=61$  and  $63$  [2,9,28,42]. We note that the  $[404]9/2$  orbital which is near the Fermi level for  $N=60$  has, to our knowledge, not yet been identified in any odd- $N$  nucleus in the  $A \approx 100$  region. Its observation in  $N=59$  isotones is difficult due to the fact that the lowest-lying states are spherical [1]. It has,

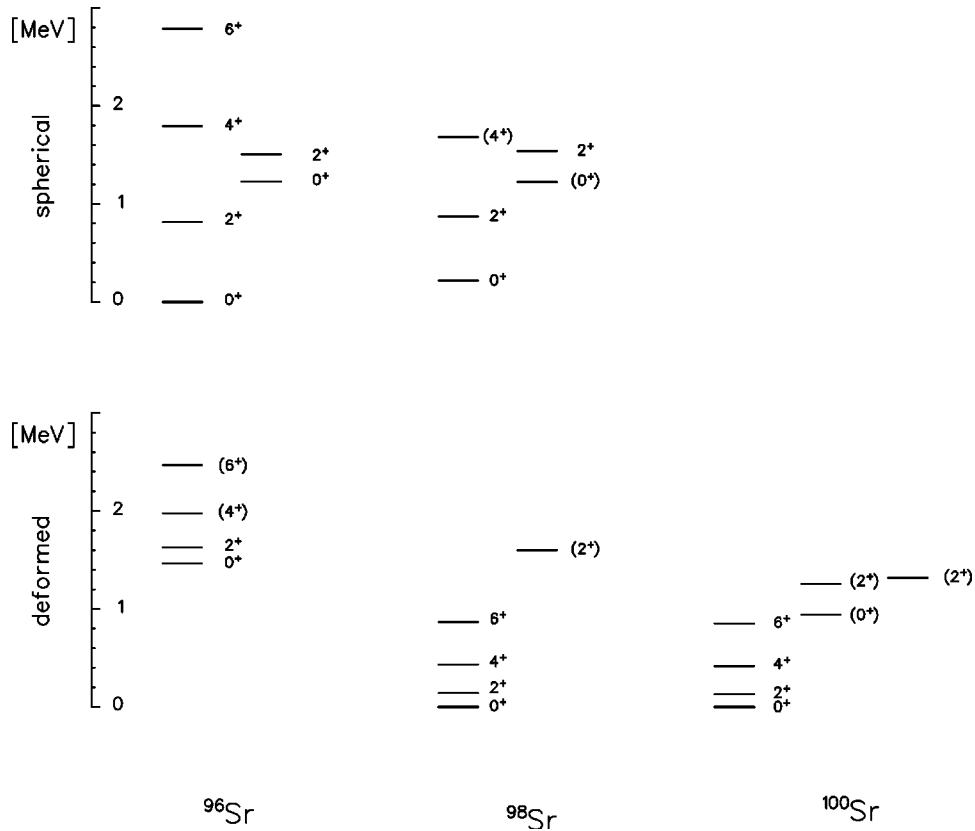


FIG. 8. Level systematics of even-even neutron-rich Sr isotopes in the  $N=58$  and  $60$  region of shape coexistence [8,1,3,9,21]. The interpretation for  $^{98}\text{Sr}$  is proposed on basis of analogies discussed in the text. However, the levels shown as the  $4^+$  and  $6^+$  states of the excited deformed band in  $^{96}\text{Sr}$  were not interpreted as such in a more recent prompt-fission study [2]. Levels in  $^{100}\text{Sr}$  are all assumed to be deformed, since the lowering of the deformed minimum is expected to continue until neutron midshell; however this was not established experimentally [39].

nevertheless, been invoked to account for isomers and band heads in the  $N=60$  isotones  $^{99}\text{Y}$  and  $^{100}\text{Zr}$  via the  $\nu[404]9/2 \otimes \nu[411]3/2$  configuration [11,12]. We therefore expect to find the lowest-lying two-quasiparticle states by coupling an unpaired  $[404]9/2$  neutron to the other one promoted on the next  $[411]3/2$  and  $[532]5/2$  orbitals. Among others, this produces  $3^+$  and  $2^-$  levels, which seem to correspond to the experimental levels at 1838 and 2124 keV, respectively. In this case, it follows that the 2231-keV level of even parity cannot be the  $K+1$  level of a band on the 2124-keV level.

These qualitative considerations are indeed supported by the Monte Carlo calculations, see Table VII. The lowest two-quasineutron band head originates from the  $[404]9/2 \otimes [411]3/2$  configuration calculated at 1.77 MeV. The next one corresponds to the  $[404]9/2 \otimes [532]5/2$  configuration at 2.11 MeV. The next states originate from the coupling of the  $[541]3/2$  hole orbital to the  $[411]3/2$  and  $[532]5/2$  levels. They are calculated near 2.5 MeV. There are, however, no experimental states with enough evidence for these configurations. The strongly  $\beta$ -fed 2231-keV level is linked to the 2124-keV level, assuming a  $2^-$  state in the following, by the 107-keV transition of low multipolarity. The absence of transitions to  $0^+$  states, rather favors  $I^\pi = 3^+$  over  $2^+$ . The second calculated  $3^+$  level involves cre-

ation of a  $\nu[422]3/2$  hole and promotion of the neutron to the  $\nu[411]3/2$  orbital. Local systematics of  $\beta$ -decay properties of odd-proton nuclei indeed shows that levels including the  $[422]3/2$  neutron orbital are strongly populated. The configuration is, however, calculated at 3.09 MeV, which is considerably higher than the experimental level. It could be lowered by moving the  $[422]3/2$  hole orbital upward, but this has not been possible within reasonable modifications of the Woods-Saxon potential parameters.

One should keep in mind that the accuracy of this theoretical prediction is affected by the single-particle level scheme, by spin-spin shifts which have been neglected, as well as by the monopole pairing approximation. However, the relative positions of the band-head levels are much less influenced by these approximations than their absolute energies. Consequently, the above proposed configurations for the 1838- ( $3^+$ ) and 2124-keV ( $2^-$ ) levels appear to be plausible.

### C. Ground states and isomers of $^{98}\text{Rb}$ and $^{100}\text{Y}$

The ground state of  $^{97}\text{Rb}$  has been measured by laser spectroscopy to be deformed and have  $I=3/2$  [43]. It is interpreted as the  $[431]3/2$  proton orbital. So far, there is

TABLE VIII. Hindrances of transitions depopulating isomers in the  $A \approx 100$  region identified by on-line mass separation (no lifetime has been reported for the band heads in  $^{100}\text{Zr}$  and  $^{102}\text{Zr}$  observed in prompt fission). Final states have  $K=0$  (even-even nuclei) and  $K=5/2$  ( $^{99}\text{Y}$ ). The figure between brackets after the transition energy in keV is the experimental branching ratio.

Isomer	Transition	To	$H$	$h$
$^{98}\text{Sr}$ , 1838 keV, 7.1 ns ( $3^+$ ) <sup>a</sup>	1693 (0.96)	$2^+$	$1.5 \times 10^6$	$1.2 \times 10^3$
	1404 (0.04)	$4^+$	$2.3 \times 10^7$	$4.8 \times 10^3$
$^{99}\text{Y}$ , 1655 keV, 1.4 ns ( $11/2^+$ ) <sup>b</sup>	1539 (0.7)	$7/2^+$	$3.9 \times 10^5$	$6.2 \times 10^2$
	1371 (0.3)	$9/2^+$	$5.4 \times 10^5$	$7.4 \times 10^2$
$^{99}\text{Y}$ , 2142 keV, 8.6 $\mu\text{s}$ ( $17/2^+$ ) <sup>c</sup>	1435 (0.13)	$13/2^+$	$2.0 \times 10^7$	$6.7 \times 10^1$
	1166 (0.14)	$15/2^+$	$4.4 \times 10^9$	$8.5 \times 10^1$
	882 (0.17)	$17/2^+$	$1.5 \times 10^9$	$6.8 \times 10^1$
	546 (0.07)	$19/2^+$	$8.8 \times 10^8$	$6.2 \times 10^1$
$^{100}\text{Sr}$ , 1619 keV, 85 ns ( $4^-$ ) <sup>d</sup>	1202 (0.9)	$4^+$	$5.2 \times 10^8$	$8.0 \times 10^2$

<sup>a</sup> $\nu[404]9/2 \otimes \nu[411]3/2$ , proposed in this work.

<sup>b</sup> $\pi[422]5/2 \otimes \nu[404]9/2 \otimes \nu[411]3/2$ , the broken neutron pair is coupled to  $3^+$  [12].

<sup>c</sup> $\pi[422]5/2 \otimes \nu[404]9/2 \otimes \nu[411]3/2$ , the broken neutron pair is coupled to  $6^+$  [12].

<sup>d</sup> $\nu[411]3/2 \otimes \nu[532]5/2$  from Ref. [13]. This configuration was also suggested for the 1821-keV level in  $^{102}\text{Zr}$  [9–11].

no experimental information about excited levels in deformed Rb isotopes. The respective  $3/2^+$  and  $5/2^+$  ground states of  $^{97}\text{Rb}$  and  $^{99}\text{Y}$  are reproduced by the calculated proton single-particle levels. One may attempt to predict the  $^{98}\text{Rb}$  ground state with the help of the Gallagher-Moszkowski rule [44]. It should result from coupling the lowest-lying quasiparticles with their relative orientations such as to further minimize the total energy. This simple rule gives a rather strong argument for the ground state of  $^{98}\text{Rb}$  to be the higher-spin  $I=(3,4)$  level, i.e., the 96-ms activity with either  $\pi[431]3/2 \otimes \nu[411]3/2$  ( $K^\pi=3^+$ ) or  $\pi[431]3/2 \otimes \nu[532]5/2$  ( $K^\pi=4^-$ ). For these configurations, even parity, which experimentally is the most probable one, is consistent with  $I=3$  only. We therefore tentatively propose  $I^\pi=3^+$  for the  $^{98}\text{Rb}$  ground state. Many configurations could be invoked for low-spin levels, either involving low-lying orbitals, but unfavored by their coupling (e.g.,  $0^+$  and  $1^-$  with the ones above), or with energy-favored coupling but higher lying. Consequently, in the absence of experimental spin assignment, it is not possible to propose a configuration for the  $I=(0,1)$   $^{98}\text{Rb}$  level corresponding to the 114-ms activity.

The feeding of the  $4^+$  state of the g.s. band in  $^{100}\text{Zr}$  limits the spin for the high-spin  $^{100}\text{Y}$  level to  $I=(3,4,5)$ , but the logft value is not low enough to ensure even parity. We would expect the  $\pi[422]5/2 \otimes \nu[411]3/2$  ( $K^\pi=4^+$ ) and  $\pi[422]5/2 \otimes \nu[532]5/2$  ( $K^\pi=5^-$ ) configurations as potential candidates for  $^{100}\text{Y}$ .

TABLE IX. Inertial parameters  $a = \hbar^2/2J$  (in keV) for some two QP bands. They have been extracted from the lowest-spin levels, except for Zr isotopes where the experimental values are from prompt fission. Note the different interpretations for band heads in Zr isotopes.

Nucleus	Band		Configuration	$\hbar^2/2J$	Ref.
	head	$K^\pi$			
$^{98}\text{Sr}$	1838	( $3^+$ )	$\nu[411]3/2 \otimes \nu[404]9/2$	17.6	this work
$^{100}\text{Zr}$	2260	( $5^-$ )	$\pi[422]5/2 \otimes \pi[303]5/2$	18.3	[10]
		( $6^+$ )	$\nu[411]3/2 \otimes \nu[404]9/2$	15.7	[11]
$^{100}\text{Sr}$	1619	( $4^-$ )	$\nu[411]3/2 \otimes \nu[532]5/2$	16.2	[13]
$^{102}\text{Zr}$	1821	(4 <sup>-</sup> )	$\pi[422]5/2 \otimes \pi[301]3/2$	16.3	[10]
			$\nu[411]3/2 \otimes \nu[532]5/2$	[11]	
$^{98}\text{Y}$	600	$1^+$	$\pi[422]5/2 \otimes \nu[422]3/2$	16.5	[23]
$^{100}\text{Y}$	10	$1^+$	$\pi[422]5/2 \otimes \nu[411]3/2$	16.1	[17]
$^{102}\text{Nb}$	0	$1^+$	$\pi[422]5/2 \otimes \nu[411]3/2$	16.1	[17]

## V. CONCLUSION

Our new data lead to an important revision of the level scheme of  $^{98}\text{Sr}$ . By analogy with  $^{96}\text{Sr}$  we propose an interpretation of the 1224- and 1539-keV levels as a  $0^+$  and  $2^+$  pairs of states due to proton-pair excitations. This implies that the  $Z=40$  spherical subshell is still present. Therefore, states of weakly collective character coexist with strongly deformed levels at  $N=60$  in  $^{98}\text{Sr}$ . This interpretation is only based on comparisons of level energies and branching ratios. It would therefore be essential to perform detailed measurements in order to determine spins and parities as well as transition rates, including those of  $E0$  transitions, before the nature of the low-lying levels can be elucidated unambiguously.

The isomeric level at 1838 keV in  $^{98}\text{Sr}$  is identified as a  $K=3$  two-quasiparticle level, with probable even parity. A cascade of 140- and 175-keV transitions forms a band structure. It is, however, difficult to understand why a corresponding level structure could not be identified in the decay of  $^{100}\text{Y}$  to  $^{100}\text{Zr}$ .

A consistent treatment of the pairing interaction within the quantum Monte Carlo and Monte Carlo projection methods allowed for theoretical prediction of the band-head excitation energies of two-quasiparticle rotational bands in  $^{98}\text{Sr}$ . The isomer at 1838 keV is firmly suggested to be associated with the  $\nu[404]9/2 \otimes \nu[411]3/2$  ( $K^\pi=3^+$ ) configuration. In addition, there is fair evidence that the new level at 2124 keV is associated with the  $\nu[404]9/2 \otimes \nu[532]5/2$  ( $K^\pi=2^-$ ) configuration. These findings further stress the importance of the  $[404]9/2$  neutron orbital at the largest deformations in the  $N=60$  region. This orbital was first invoked to account for isomers in  $^{99}\text{Y}$ , and more recently for the 2260-keV band head in  $^{100}\text{Zr}$ . The nature of this latter level is still unclear and cannot be elucidated by the present calculation. This is because the occupation of proton levels above the  $Z=38$  deformed gap allows coexistence of two-quasiproton and two-quasineutron levels in the same excitation energy range in Zr isotopes.



## ACKNOWLEDGMENTS

This work was supported by the German Bundesministerium for Education and Research (BMBF), the German Service for Exchange with Foreign Countries (DAAD), the Academy of Finland, the Ministerio de Educación, Cultura y Deportes de España, and the Training and Mobility of Researchers Program (TMR) of the European Union. We wish to thank Dr. P. Jones for help in recovering the data from the

experiment at the ISOLDE facility, and Dr. P. Dendooven for operation of the IGISOL mass separator. We are also much indebted to Professor K. Heyde for his illuminating comments about the origin of intruder states and careful reading of the manuscript. One of the authors (G.L.) wishes to thank the GANIL and IReS laboratories for giving the opportunity to complete this work during his leave of absence from Jyväskylä.

- 
- [1] G. Lhersonneau, B. Pfeiffer, K.-L. Kratz, J. Äystö, T. Enqvist, P. P. Jauho, A. Jokinen, J. Kantele, M. Leino, J. M. Parmonen, and H. Penttilä, *Phys. Rev. C* **49**, 1379 (1994).
- [2] W. Urban, J. L. Durell, A. G. Smith, W. R. Phillips, M. A. Jones, B. J. Varley, T. Rząca-Urban, I. Ahmad, L. R. Morss, M. Bentaleb, and N. Schulz, *Nucl. Phys.* **A689**, 605 (2001).
- [3] K. Becker, G. Jung, K.-H. Kobras, H. Wollnik, and B. Pfeiffer, *Z. Phys. A* **319**, 193 (1984).
- [4] F. K. Wohn, J. C. Hill, C. B. Howard, K. Sistemich, R. F. Petry, R. L. Gill, H. Mach, and A. Piotrowski, *Phys. Rev. C* **33**, 677 (1986).
- [5] H. Ohm, G. Lhersonneau, K. Sistemich, B. Pfeiffer, and K.-L. Kratz, *Z. Phys. A* **327**, 483 (1987).
- [6] F. Buchinger, E. B. Ramsay, E. Arnold, W. Neu, R. Neugart, K. Wendt, R. Silverans, E. Lievens, L. Vermeeren, D. Berdichewsky, R. Fleming, and D. W. L. Sprung, *Phys. Rev. C* **41**, 2883 (1990).
- [7] H. Mach, M. Moszynski, R. L. Gill, G. Molnár, F. K. Wohn, J. A. Winger, and J. C. Hill, *Phys. Rev. C* **41**, 350 (1990).
- [8] J. L. Wood, E. F. Zganjar, C. De Coster, and K. Heyde, *Nucl. Phys.* **A651**, 323 (1999).
- [9] J. H. Hamilton, A. V. Ramayya, S. J. Zhu, G. M. Ter-Akopian, Yu. Oganessian, J. D. Cole, J. O. Rasmussen, and M. A. Stoyer, *Prog. Part. Nucl. Phys.* **35**, 635 (1995).
- [10] J. H. Hamilton, Q. H. Lu, S. J. Zhu, K. Butler-Moore, A. V. Ramayya, B. R. S. Babu, L. K. Peker, W. C. Ma, T. N. Ginter, J. Kormicki, D. Shi, J. K. Deng, J. O. Rasmussen, M. A. Stoyer, S. Y. Chu, K. E. Gregorich, M. F. Mohar, S. Prussin, J. D. Cole, R. Aryaeinejad, N. R. Johnson, I. Y. Lee, F. K. McGowan, G. M. Ter-Akopian, and Yu. Ts. Oganessian, in *Proceedings of the International Conference on Exotic Nuclei and Atomic Masses, Arles, France, 1995*, edited by M. de Saint Simon and O. Sorlin (Frontières, Gif sur Yvette, 1995), p. 487.
- [11] J. L. Durell, W. R. Phillips, C. J. Pearson, J. A. Shannon, W. Urban, B. J. Varley, N. Rowley, K. Jain, I. Ahmad, C. J. Lister, L. R. Morss, K. L. Nash, C. W. Williams, N. Schulz, E. Lubkiewicz, and M. Bentaleb, *Phys. Rev. C* **52**, R2306 (1995).
- [12] R. A. Meyer, E. Monnard, J. A. Pinston, F. Schussler, I. Ragnarsson, B. Pfeiffer, H. Lawin, G. Lhersonneau, T. Seo, and K. Sistemich, *Nucl. Phys.* **A439**, 510 (1985).
- [13] B. Pfeiffer, G. Lhersonneau, H. Gabelmann, K.-L. Kratz, and the ISOLDE Collaboration, *Z. Phys. A* **353**, 1 (1995).
- [14] B. Pfeiffer and K.-L. Kratz, in *Proceedings of the International Workshop on Nuclear Structures of the Zirconium Region, Bad Honnef, Germany, 1988*, edited by J. Eberth, R. A. Meyer, and K. Sistemich (Springer-Verlag, Berlin, 1988), p. 368.
- [15] B. Pfeiffer, V. Harms, E. Monnard, and K.-L. Kratz, in *Nuclei Far From Stability*, edited by Ian S. Townes, AIP Conf. Proc. No. 164 (AIP, New York, 1988), p. 403.
- [16] R. Capote, E. Mainegra, and A. Ventura, *J. Phys. G* **24**, 1113 (1998).
- [17] J. K. Hwang, A. V. Ramayya, J. Gilat, J. H. Hamilton, L. K. Peker, J. O. Rasmussen, J. Kormicki, T. N. Ginter, B. R. S. Babu, C. J. Beyer, E. F. Jones, R. Donangelo, S. J. Zhu, H. C. Griffin, G. M. Ter-Akopyan, Yu. Ts. Oganessian, A. V. Daniel, W. C. Ma, P. G. Varmette, J. D. Cole, R. Aryaeinejad, M. W. Drigert, and M. A. Stoyer, *Phys. Rev. C* **58**, 3252 (1998).
- [18] B. Pfeiffer, G. Lhersonneau, H. Gabelmann, K.-L. Kratz, and the ISOLDE and OSTIS Collaboration, Annual Report 1995, Institute für Kernchemie, Mainz, 24, 1996, URL: <http://www.kernchemie.uni-mainz.de/~pfeiffer/jb96sr98.html>
- [19] G. Lhersonneau, H. Gabelmann, N. Kaffrell, K.-L. Kratz, B. Pfeiffer, K. Heyde, and the ISOLDE Collaboration, *Z. Phys. A* **337**, 143 (1990).
- [20] P. Dendooven, S. Hankonen, A. Honkanen, M. Huhta, J. Huikari, A. Jokinen, V. S. Kolhinen, G. Lhersonneau, A. Nieminen, M. Oinonen, H. Penttilä, K. Peräjärvi, J. C. Wang, and J. Äystö, in *Proceedings of the 2nd International Workshop on Nuclear Fission and Fission-Product Spectroscopy, Seyssins, France, 1998*, edited by G. Fioni, H. Faust, S. Oberstedt, and F. J. Hamsch, AIP Conf. Proc. No. 447 (AIP, Woodbury, NY, 1998), p. 135.
- [21] R. B. Firestone and V. S. Shirley, *Table of Isotopes*, 8th ed. (Wiley, New York, 1996).
- [22] K.-L. Kratz, A. Schröder, H. Ohm, M. Zendel, H. Gabelmann, W. Ziegert, P. Peuser, G. Jung, B. Pfeiffer, K.-D. Wünsch, H. Wollnik, C. Ristori, and J. Crançon, *Z. Phys. A* **306**, 239 (1982).
- [23] H. Mach, M. Moszynski, R. L. Gill, F. K. Wohn, J. A. Winger, J. C. Hill, G. Molnár, and K. Sistemich, *Phys. Lett. B* **230**, 21 (1989).
- [24] F. Schussler, J. A. Pinston, E. Monnard, A. Moussa, G. Jung, E. Koglin, B. Pfeiffer, R. V. Janssens, and J. van Klinken, *Nucl. Phys.* **A339**, 415 (1980).
- [25] J. Äystö, P. P. Jauho, Z. Janas, A. Jokinen, J. M. Parmonen, H. Penttilä, P. Taskinen, R. Béraud, R. Duffait, A. Emsallem, J. Meyer, M. Meyer, N. Redon, M. E. Leino, K. Eskola, and P. Dendooven, *Nucl. Phys.* **A515**, 365 (1990).
- [26] R. R. Chasman, *Z. Phys. A* **339**, 11 (1991).
- [27] J. Skalski, S. Mizutori, and W. Nazarewicz, *Nucl. Phys.* **A617**, 282 (1997).

- [28] M. C. A. Hotchkis, J. L. Durell, J. B. Fitzgerald, A. S. Mowbray, W. R. Philips, I. Ahmad, M. Carpenter, R. V. F. Janssens, T. L. Khoo, E. F. Moore, L. Morss, Ph. Benet, and D. Ye, Nucl. Phys. **A530**, 111 (1991).
- [29] W. Nazarewicz, J. Dudek, R. Bengtsson, T. Bengtsson, and I. Ragnarsson, Nucl. Phys. **A435**, 397 (1985).
- [30] V. V. Pashkevich, Nucl. Phys. **A169**, 275 (1971).
- [31] J. Dudek, Z. Szymanski, and T. Werner, Phys. Rev. C **23**, 920 (1981).
- [32] J. Dudek, Z. Szymanski, T. Werner, A. Faessler, and C. Lima, Phys. Rev. C **26**, 1712 (1982).
- [33] Z. Lojewski, B. Nerlo-Pomorska, K. Pomorski, and J. Dudek, Phys. Rev. C **51**, 601 (1995).
- [34] C. J. Gallagher, Jr., Phys. Rev. **126**, 1525 (1962).
- [35] V. G. Soloviev, *Teoriya atomnovo yadra: Yadernie modeli (Nuclear theory: Nuclear models in Russian)* (Energoatomizdat, Moscow, Russia, 1981), pp. 180,181, Eqs. (5.97) and (5.97').
- [36] H. J. Lipkin, Ann. Phys. (N.Y.) **9**, 272 (1960); Y. Nogami, Phys. Rev. **134**, B313 (1964); H. C. Pradhan, Y. Nogami, and J. Law, Nucl. Phys. **A201**, 357 (1973).
- [37] N. Cerf, Nucl. Phys. **A564**, 383 (1993).
- [38] R. Capote and A. Gonzalez, Phys. Rev. C **59**, 3477 (1999).
- [39] G.-L. Long, S.-J. Zhu, L. Tian, and H.-Z. Sun, Chin. J. Nucl. Phys. **17**, 149 (1995); Phys. Lett. B **345**, 351 (1995).
- [40] G. Lhersonneau, B. Pfeiffer, H. Gabelmann, K.-L. Kratz, and the ISOLDE Collaboration Phys. Rev. C **63**, 054302 (2001).
- [41] K. Heyde, C. De Coster, B. Decroix, J. L. Wood, and E. F. Zganjar, in *Proceedings of the 9th International Symposium on Capture Gamma-Ray Spectroscopy and Related Topics, Budapest, Hungary, 1996*, edited by G. L. Molnár, T. Belgya, and Zs. Revay (Springer-Verlag, Budapest, 1997), p. 123.
- [42] G. Lhersonneau, P. Dendooven, A. Honkanen, M. Huhta, M. Oinonen, H. Penttilä, J. Äystö, J. Kurpeta, J. R. Persson, and A. Popov, Phys. Rev. C **54**, 1592 (1996).
- [43] C. Thibault, F. Touchard, S. Büttgenbach, R. Klapisch, M. de Saint-Simon, H. T. Duong, P. Jacquinet, P. Juncar, S. Liberman, P. Pillet, P. Pinard, J. L. Vialle, A. Pesnelle, and G. Huber, Phys. Rev. C **23**, 2720 (1981).
- [44] C. J. Gallagher, Jr. and S. A. Moszkowski, Phys. Rev. **111**, 1282 (1958).